

# Nanocrystalline/nanosized Fe<sub>3</sub>O<sub>4</sub> particles obtained by heat treatment and mechanical milling

T. F. MARINCA\*, I. CHICINAȘ, O. ISNARD<sup>a</sup>, B. V. NEAMȚU

*Materials Sciences and Engineering Department, Technical University of Cluj-Napoca, Cluj-Napoca 400641, Romania*

*<sup>a</sup>Institut Néel, CNRS, and Université Joseph Fourier, Grenoble 38042 Grenoble, France*

The nanocrystalline/nanosized magnetite – Fe<sub>3</sub>O<sub>4</sub> particles have been obtained by heat treatment mixture of hematite - α-Fe<sub>2</sub>O<sub>3</sub> and elemental Fe stoichiometric mixture and subsequent mechanical milling procedure. The powder has been investigated by X-ray diffraction, laser particle size analysis and magnetic studies. The mean crystallite size of the Fe<sub>3</sub>O<sub>4</sub> rapidly decrease by increasing the milling time. After 5 minutes it is about 14 nm. Prolonged milling times lead to the oxidation of magnetite into hematite. The particles size presents a rapid decrease in the first stage of milling, up to 3 minutes of milling. The specific surface and the number of nanometric particles increase also in the first stage of milling. The magnetisation decreases for milling times longer than 15 minutes and tends to become unsaturated.

(Received October 31, 2014; accepted May 7, 2015)

*Keywords:* Magnetite, Iron oxide, Nanocrystalline, Mechanical milling, Nanoparticles

## 1. Introduction

Iron oxides, (wüstite - FeO, magnetite - Fe<sub>3</sub>O<sub>4</sub>, hematite - α-Fe<sub>2</sub>O<sub>3</sub>, maghemite - γ-Fe<sub>2</sub>O<sub>3</sub>) are of interest for research and also have applications in various field of industry [1-5]. Among these oxides, the magnetite is probably the most studied. The magnetite is crystallographically isomorphous with the maghemite which is the allotropic form of this. The magnetite (FeFe<sub>2</sub>O<sub>4</sub>) crystallises in cubic spinel structure Fd-3m characteristic for the soft ferrites (MeFe<sub>2</sub>O<sub>4</sub>). Typical, as the large part of the soft ferrite, the iron ferrite - Fe<sub>3</sub>O<sub>4</sub> is ferrimagnetic at room temperature [6-7]. The magnetite ferrimagnetism derive from the arrangement of the Fe<sup>2+</sup> and Fe<sup>3+</sup> cations into the cubic spinel structure. The Fe<sup>2+</sup> and half of Fe<sup>3+</sup> cations are located into octahedral sites and the other half of the Fe<sup>3+</sup> cations are located into the tetrahedral sites. The octahedral sites form a magnetic sublattice that is coupled anti-parallel with the other magnetic sublattice, the tetrahedral one [6]. The synthesis of magnetite particles in nanocrystalline/nanosized state is nowadays one of the interesting subjects of the research aiming to optimise the various types of applications from magnetic storage devices, magnetic refrigeration system, mineral separation and catalysis to drug delivery, immunoassay, hyperthermia, magnetic resonance imaging, cancer therapy or magnetic cell separation [8-11]. Several synthesis routes such as microwave-solvothermal [12], coprecipitation [13], hydrothermal [14] or mechanosynthesis [15] can be used for obtaining magnetite in nanocrystalline/nanosized state. Among the synthesis routes, the mechanosynthesis is one of most versatile technique to obtain nanocrystalline/nanosized magnetite particles. In order to synthesize obtain such particles by techniques of mechanosynthesis various precursors such as

magnetite wet milled in methanol [15], magnetite dry milled [16], iron milled in water [17] or hematite and iron [18] can be used.

The paper presents the synthesis of magnetite particles by a new route combining heat treatment and mechanical milling to produce polycrystalline and nanocrystalline/nanosized states. It was investigated the influence of the synthesis conditions to the structural and magnetic characteristics and particles size.

## 2. Experimental

A stoichiometric mixture of hematite - Fe<sub>2</sub>O<sub>3</sub> (Alpha Aesar) and iron - Fe (Höganäs) powders was used for the synthesis of Fe<sub>3</sub>O<sub>4</sub>. The Fe<sub>2</sub>O<sub>3</sub> and Fe mixture has been homogenized in a turbula type apparatus for 15 minutes. This obtained blend has been subjected to the annealing in a tubular furnace in argon at 600 °C for 10 hours. For the mechanical milling procedure a high energy planetary ball mill (Fritsch, Pulverisette 6) was used. The milling process was carried out in air using a vial of 250 ml volume and balls with the diameter of 14 mm. The milling times were chosen as follow: 1, 3, 5, 15, 30, 60, 120, 180 and 240 minutes. A balls to powder mass ratio of 20:1 was chosen. The milling was performed at 300 rpm. The structural investigations were made by X-ray diffraction technique. A Siemens D5000 diffractometer which operates in reflection with CoKα radiation was used for the X-ray diffraction. The X-ray diffraction patterns were recorded in an angular range of 2θ=20-100°. The mean crystallites size and the lattice strain were calculated by X'Pert HighScore software. The lattice parameter was calculated using Celref program. The magnetisation curves were recorded at 300 K using the extraction sample

method in a continuous magnetic field of up to 10 T. The saturation magnetisation values were obtained from the law of approach to saturation:

$$M = M_S \left( 1 - \frac{a}{H} - \frac{b}{H^2} \right) + \chi H \quad (1)$$

The particle size distribution, specific surface and  $d_n$  parameters determinations were performed by a Laser Particle Size Analyser (Fritsch Analysette 22 – Nanotec). The  $d_n$  diameter represents the particles size diameter for which n% volume percent of particles are smaller than  $d_n$ . The apparatus has an analysis range of 10 nm to 2000  $\mu$ m. Prior to this laser particles analysis, the samples were subjected to the dis-agglomeration in ultrasonic bath.

### 3. Results and discussion

Fig. 1 presents the comparison of X-ray diffraction patterns of the un-milled and milled magnetite samples. In the diffraction pattern of the un-milled sample are noticed the peaks of magnetite, Fe<sub>3</sub>O<sub>4</sub>, cubic spinel structure, thus indicating the formation of this phase by annealing of the stoichiometric mixture of Fe and Fe<sub>2</sub>O<sub>3</sub> [19]. It can be remarked that the magnetite presents some FeO - wüstite and Fe impurities, some peaks of these phases are also noticed in the diffraction pattern of un-milled sample.

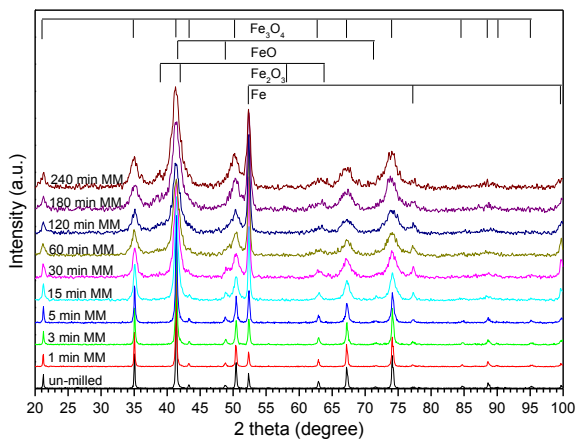


Fig. 1. X-ray diffraction patterns of the magnetite un-milled and milled for 1, 3, 5, 15, 30, 60, 120, 180 and 240 minutes samples.

The mechanical milling up to 30 minutes leads to the preservation of Fe<sub>3</sub>O<sub>4</sub> phase (alongside of impurities), no new peaks can be observed. After 30 minutes of milling the most intense peak of  $\alpha$ -Fe<sub>2</sub>O<sub>3</sub> is detected (at about 38.7°). This is assigned to some powder oxidation during milling in air. It worth to be mentioned that the formation of some maghemite ( $\gamma$ -Fe<sub>2</sub>O<sub>3</sub>) cannot be excluded. This is difficult to be evidenced by X-ray diffraction due to the crystallographic isomorphism with magnetite. The amount of hematite increases by increasing the milling time up to

240 minutes as indicated by the increase of the Bragg peaks. Increasing the milling time leads the broadening of the peaks as a result of the crystallite size decrease and the internal stress induced by mechanical milling.

The evolution of the mean crystallite size and lattice strain versus milling time is shown in Fig. 2. It can be noticed that the crystallite size is reduced down to 90 nm for only 5 minutes of milling. For the un-milled sample was impossible to determine the mean crystallite size by the same method due to the too large size of the crystallite. The mean particles size measured by laser particles size analyser is at 2.7  $\mu$ m. Such particles have crystallite in micrometers range and then, in only 5 minutes the crystallites size presents an efficient decrease. After 15 minutes of milling the magnetite crystallites are at about 14 nm and continuously refine up to 6 nm by increasing the milling time up to 240 minutes. The lattice strain continuously increases upon increasing the milling time. The lattice strain doubled during milling of the sample from 15 minutes to 240 minutes. The refinement of the crystalline size and the increase of the lattice strain are typically of that reported for milled ferrite [20, 21].

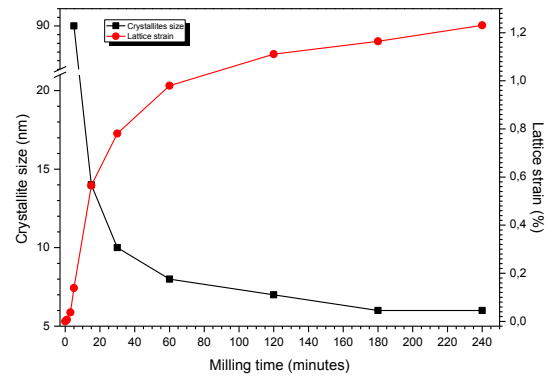


Fig. 2. Evolution of the mean crystallite size and lattice strain versus milling time.

Fig. 3 shows the evolution of the  $d_{10}$ ,  $d_{50}$  and  $d_{90}$  parameters of the magnetite particles as a function of milling time. In the first minutes of milling (up to 3 minutes) the  $d_{10}$ ,  $d_{50}$  and  $d_{90}$  parameters of magnetite particles present a large decrease. The  $d_{10}$  is at 800 nm,  $d_{50}$  at 1.8  $\mu$ m and  $d_{90}$  at 7.8  $\mu$ m. The decrease of these parameters indicates the predominance of the fragmentation process in this first stage of milling. After 3 minutes of milling and up to for 15 minutes of milling it is remarkable increase of the  $d_{90}$  parameter is observed (up to 23.7  $\mu$ m) suggesting the predominance of the cold welding processes. In the mean time the  $d_{10}$  and  $d_{50}$  have a slight increase up to 900 nm and 0.9  $\mu$ m respectively. The cold welding process tend to become predominate after 3 minutes of milling. The  $d_{50}$  increase continuously up to 120 minutes of milling and  $d_{90}$  parameter has a slight variation at this milling time suggesting the predominance of the cold welding processes. The  $d_{10}$  parameter is almost constant up to the end of the milling process. The  $d_{50}$  and  $d_{90}$  are also constant by increasing the milling time from

120 up to 240 minutes of milling. The constancy of all these three parameters is due to the reaching of a quasi-equilibrium between fragmentation and cold welding process [22].

The evolution of the specific surface area of the particles and of the amount of the nanosized particles with diameter smaller than 500 nm is presented in Fig. 4. Both have similar evolution. As it was expected from the evolution of the  $d_{10}$ ,  $d_{50}$  and  $d_{90}$  parameters during the first minutes of milling, the specific surface increases. Also, in the same milling period it increases the amount of particles with the diameter smaller than 500 nm. The percentage of nanosized particles and the specific surface decrease during the dominance of cold welding process up to 15 minutes of milling. Indeed, the cold welding can lead to the decrease of the specific surface. The specific surface exhibit another increase with increase of the milling from 15 to 30 minutes. In this milling, the  $d_{50}$  and  $d_{90}$  do not suffer significant changes, but the amount of the nanosized particles significantly increases and also the  $d_{10}$  slightly increases. This increase is assigned to the change of the amount of the nanosized particles and the diminution of other fine particles ( $d_{10}$  decrease). The decrease of the specific surface is in good correlation with the evolution of the  $d_{10}$ ,  $d_{50}$  and  $d_{90}$  parameters and nanosized particles evolution. One can observe that the significant increase of the amount of the nanosized particles (from 4.1 up to 7.5 %) goes together with and a slight diminution of the  $d_{50}$  and  $d_{90}$  parameter leads to an increase of the specific surface.

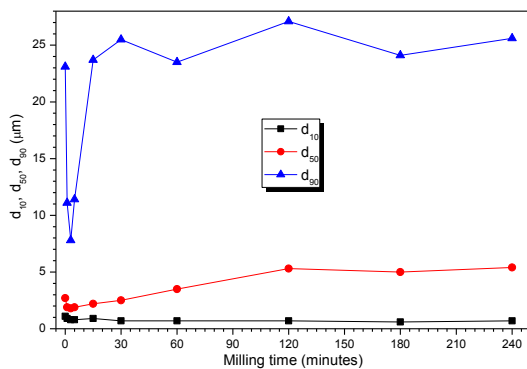


Fig. 3. Evolution of the  $d_{10}$ ,  $d_{50}$  and  $d_{90}$  parameters of the magnetite particles versus milling time.

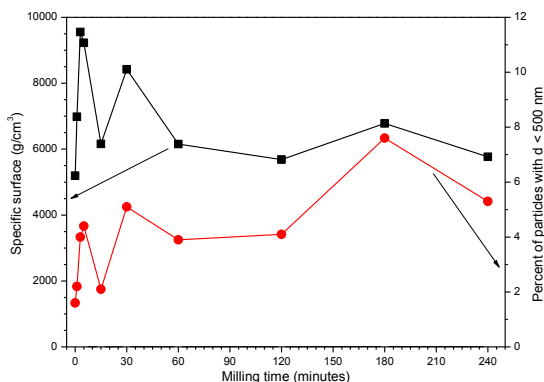


Fig. 4. Evolution of the specific surface area of the particles and the amount of particles with diameter smaller than 500 nm.

One can remark that in the case of the particles subjected to mechanical milling the  $d_n$  parameters and the amount of nanometric particles may be underestimated. This may originate from the incomplete separation of the bonded particles during the ultrasonic bath separation procedure. Therefore, taken into account the fragile character of the ferrite and the incomplete separation during the ultrasonic procedure one can assume that the particles are formed by multiple particles that are bonded [21]. The large particles can have nanoparticles bonded on the surface and also the very fine particles should consist in bonded nanoparticles.

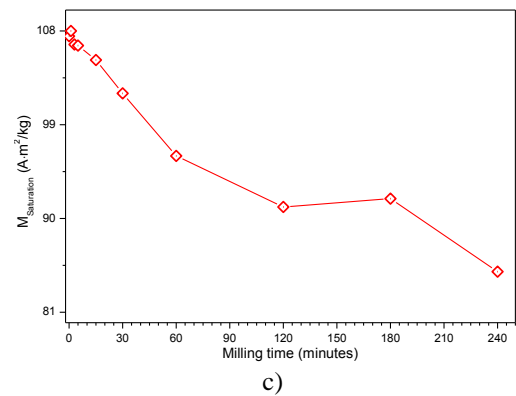
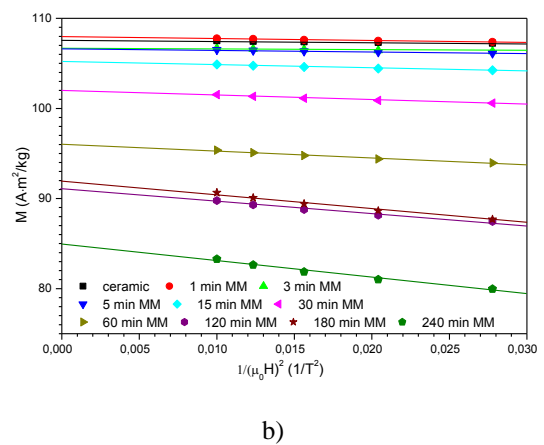
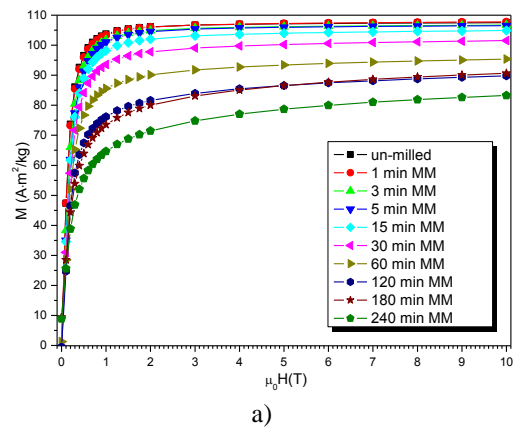


Fig. 5. a) Magnetite particles magnetisation curves recorded at 300 K b) magnetisation versus  $1/H^2$  plots derived from the room temperature magnetisation curves and c) evolution of the saturation magnetisation versus milling time.

The formation of the hematite phase for prolonged milling time, proved by X-ray diffraction, can be explained by the large particles specific surface area that can have a lot of atmospheric oxygen adsorbed and by the influence of the mechanical absorbed energy favouring oxidation.

The magnetisation curves of the magnetite particles recorded at 300 K are shown in Fig. 5. In the same figure are presented the magnetisation versus  $1/H^2$  plots deriving from the 300 K magnetisation curves and the evolution of the saturation magnetisation as a function of milling time. The curve of the un-milled sample is typical for the ferromagnetic/ferromagnetic material. The magnetite obtained in equilibrium conditions is in ferromagnetic state with the cations Fe<sup>2+</sup> located in octahedral sites and Fe<sup>3+</sup> cations equal distributed between tetrahedral and octahedral sites [6]. The magnetisation curves present similar shape and closed value up to 15 minutes of milling. For this short milling time, the milling process does not affect significantly the magnetic structure. The magnetisation decrease is less than 2.2 % (from 107.5 to 105.2 A·m<sup>2</sup>/kg). The saturation magnetisation of the samples present a significant decrease by increasing the milling time from 15 to 30 minutes and a large decrease upon further increasing the milling time up to 240 minutes. After 240 minutes of milling the saturation magnetisation reaches 84.9 A·m<sup>2</sup>/kg. This value represents only 79 % of the value of the un-milled sample. The decrease of the magnetisation is assigned to the internal stresses and spin canted effect induced during milling into the material and also to the other structural defects. In the first magnetisation curves one can observe a tendency of the magnetisation to become un-saturated with increasing of the milling time. Indeed, the magnetisation increases linearly by increasing the magnetic field. This behaviour is typical for the milled samples that present spin canted [20, 21, 23]. During mechanical milling the magnetic spins that are located on the particles surface become canted. The large spin canted effect arises for the large specific surface and the existence of the large number of nanoparticles. The magnetic moments are consequently more and more difficult to be orient for long the milling time.

#### 4. Conclusions

The nanocrystalline/nanosized magnetite – Fe<sub>3</sub>O<sub>4</sub> particles have been synthesized by a new annealing – mechanical milling combined route. As precursors for magnetite pure and low cost materials of iron and hematite have been used. Very short milling times are favourable to produce nanocrystalline/nanosized magnetite particles. A milling time of 15 minutes is enough to decrease the crystallite size from micrometers down to 14 nm. Prolonged milling times induce some oxidation process leading to the formation of hematite – Fe<sub>2</sub>O<sub>3</sub>. The amounts of nanometric particles and of specific surface increase by a factor two in the first 5 minutes of milling. The magnetisation exhibits slight change in the first 15 minutes of milling, but is diminished continuously by increasing the milling time up to 240 minutes and tends to become unsaturated as a result of spin canted effect. The annealing procedure needs to be improved in order to increase the purity of the as obtained magnetite. A synthesis route

involving annealing-short time mechanical milling is found to be useful for the synthesis of nanocrystalline/nanosized magnetite.

#### Acknowledgement

This paper was supported by the Post-Doctoral Programme POSDRU/159/1.5/S/137516, project co-funded from European Social Fund through the Human Resources Sectorial Operational Program 2007-2013.

#### References

- [1] R. M. Cornell, U. Schwertmann, *The iron oxides*, Wiley-VCH Verlag, KGaA, Weinheim, (2003).
- [2] A. K. Gupta, M. Gupta, *Biomaterials* **26**, 3995 (2005).
- [3] N. M. Deraz, A. Alarifi, *Ceram. Int.* **38**, 4049 (2012).
- [4] H. I. Hsiang, F. S. Yen, *Ceram. Int.* **29**, 1 (2003).
- [5] A. Kihal, B. Bouzabata, G. Fillion, D. Fruchart, *Physics Procedia* **2**, 665 (2009).
- [6] B. D. Cullity, C. D. Graham. *Introduction to Magnetic Materials*, 2<sup>nd</sup> edition, IEEE Press&Wiley, New Jersey, (2009).
- [7] A. Goldman, *Modern Ferrite Technology*, 2<sup>nd</sup> edition, Springer, Pittsburgh, (2006).
- [8] D. Wilson, M. A. Langell, *Appl. Surf. Sci.* **303**, 6 (2014).
- [9] P. Panneerselvam, N. Morad, K.A. Tan, *J. Hazard. Mater.* **186**, 160 (2011).
- [10] K. Hayashi, W. Sakamoto, T. Yogo, *J. Magn. Magn. Mater.* **321**, 450 (2009).
- [11] M. Fang, V. Ström, R.T. Olsson, L. Belova, K.V. Rao, *Nanotechnol.* **23**, 145601 (2012).
- [12] C. Li, Y. Wei, A. Liivat, Y. Zhu, *J. Zhu, Mater. Lett.* **107**, 23 (2013).
- [13] B. Peeples, V. Goornavar, C. Peeples, D. Spence, V. Parker, C. Bell, D. Biswal, G. T. Ramesh, A. K. Pradhan, *J. Nanopart. Res.* **16**, 2290 (2014).
- [14] X. Wu, J. Tang, Y. Zhang, H. Wang, *Mater. Sci. Eng., B* **157**, 81 (2009).
- [15] G. F. Goya, *Solid State Commun.* **130**, 783 (2004).
- [16] E. Bonetti, L. Del Bianco, S. Signoretti, P. Tiberto, *J. Appl. Phys.* **89**, 1806 (2001).
- [17] M. M. Can, S. Ozcan, A. Ceylan, T. Firat, *Mater. Sci. Eng., B* **172**, 72 (2010).
- [18] E. Petrovský, M. D. Alcalá, J. M. Criado, T. Grygar, A. Kapička, J. Šubrt, *J. Magn. Magn. Mater.* **210**, 257 (2000).
- [19] T. F. Marinca, B. V. Neamtu, I. Chicinaş, O. Isnard, *J. Alloys Compd.* **608**, 54 (2014).
- [20] C. N. Chinnasamy, A. Narayanasamy, N. Ponpandian, K. Chattopadhyay, H. Guérault, J-M Greneche, *J. Phys.: Condens. Matter* **12**, 7795 (2000).
- [21] T. F. Marinca, I. Chicinaş, O. Isnard, V. Popescu, *J. Am. Ceram. Soc.* **96**, 469 (2013).
- [22] C. Suryanarayana, *Mechanical Alloying and Milling*, Marcel Dekker, New York, (2004).
- [23] T. F. Marinca, I. Chicinaş, O. Isnard, V. Pop, *Optoelectron. Adv. Mater. Rapid Comm.* **5**, 39 (2011).

\*Corresponding author: traian.marinca@stm.utcluj.ro